PNAS RESEARCH ARTICLE | PLANT BIOLOGY

The nitrate transporter NRT2.1 directly antagonizes PIN7-mediated auxin transport for root growth adaptation

Yalu Wang[a,1], Zhi Yuan[a,1], Jinyi Wang[a,1], Huixin Xiao[a], Lu Wan[a], Lanxin Li[b], Yan Guo[a], Zhizhong Gong[a,c], Jiří Friml[d], and Jing Zhang[a,2]

Edited by Yi-Fang Tsay, Academia Sinica, Taipei, Taiwan; received December 15, 2022; accepted March 28, 2023

As a crucial nitrogen source, nitrate (NO_3^-) is a key nutrient for plants. Accordingly, root systems adapt to maximize NO_3^- availability, a developmental regulation also involving the phytohormone auxin. Nonetheless, the molecular mechanisms underlying this regulation remain poorly understood. Here, we identify *low-nitrate-resistant mutant* (*lonr*) in Arabidopsis (*Arabidopsis thaliana*), whose root growth fails to adapt to low-NO_3^- conditions. *lonr2* is defective in the high-affinity NO_3^- transporter NRT2.1. *lonr2* (*nrt2.1*) mutants exhibit defects in polar auxin transport, and their low-NO_3^--induced root phenotype depends on the PIN7 auxin exporter activity. NRT2.1 directly associates with PIN7 and antagonizes PIN7-mediated auxin efflux depending on NO_3^- levels. These results reveal a mechanism by which NRT2.1 in response to NO_3^- limitation directly regulates auxin transport activity and, thus, root growth. This adaptive mechanism contributes to the root developmental plasticity to help plants cope with changes in NO_3^- availability.

nitrate | auxin transport | root growth adaptation

Significance

Modulation of primary root growth is a foraging strategy adapting to NO_3^- fluctuation in soil. However, how that comes about remains unclear. Here, we identify a unique mechanism involving the interaction of two transporters specific to different substrates (NO_3^- or auxin). Our study demonstrates that the high-affinity NO_3^- transporter NRT2.1 directly associates with the auxin transporter PIN7, and antagonizes its activity depending on NO_3^- levels, thus regulating primary root elongation. Collectively, this work provides insight into the mechanisms regulating root growth adaptation in response to NO_3^- availability.

Plants are sessile and have evolved elaborated mechanisms to cope with unfavorable environmental conditions. Roots are vital organs responsible for the acquisition of resource from the soil and are thus responsive to a wide range of external stimuli. Changes in root architecture and development contribute to plant adaptation to environmental stresses. However, only a few mechanisms explaining root plasticity have been proposed.

Nitrogen is a vital macronutrient for plant growth. As the main form of inorganic nitrogen, nitrate (NO_3^-) is not only the preferred nitrogen source but also acts as a signal molecule regulating many plant physiological processes. The NO_3^- signaling cascade, which comprises a transceptor (nitrate transporter1.1, NRT1.1), protein kinases (e.g., Ca^{2+}-sensor protein kinases, CPKs), and transcription factors (e.g., NIN-like proteins, NLPs), contributes to the control of root development in response to NO_3^- availability (1–4). Furthermore, plant hormones (e.g., auxin; brassinosteroids) and signaling peptides (e.g., CLAVATA3/ESR-related, CLE; C-terminally encoded peptide, CEP) also mediate NO_3^--regulated root responses (1, 5–9).

Given the universal role of the phytohormone auxin in determining root architecture, it is not surprising that there are strong evidences supporting connections between NO_3^- and auxin. Indeed, auxin transport, signaling, and biosynthesis all participate in NO_3^--mediated root development. For instance, the NO_3^- transceptor NRT1.1 not only senses and transports NO_3^- in both high- and low-NO_3^- affinity states (switching between the two states by phosphorylation and dephosphorylation), but also facilitates auxin transport and thus inhibits lateral root development under low external NO_3^- concentrations (1, 10–12). Low NO_3^- increases auxin transport from shoots to roots and regulates plant root growth (13). NO_3^- availability transcriptionally regulates the expression of several auxin efflux carrier genes that are required for root development (14). Low NO_3^- represses auxin accumulation potentially by raising NRT1.1 protein abundance and ultimately stimulates distal stem cell differentiation in root tips (9). Dephosphorylation of the auxin efflux carrier PIN-FORMED2 (PIN2) is related to NO_3^--regulated root cell division and elongation (15). Expression of *auxin response factor8* (*ARF8*) is responsive to the NO_3^- metabolite glutamine and regulates lateral root outgrowth (16). The auxin receptor auxin-signaling F-box protein3 (AFB3) specifically coordinates primary and lateral root growth in response to external and internal NO_3^- availability (17, 18). The MADS-box transcription factor AGAMOUS-like21 (AGL21) promotes lateral root initiation and elongation by enhancing local auxin biosynthesis when NO_3^- is limited (19). The auxin biosynthesis gene *tryptophan amino-transferase related2* (*TAR2*) promotes lateral root formation under low-NO_3^- conditions (20). In summary, NO_3^- and auxin tightly interact to modulate root architecture; however, the underlying molecular mechanisms remain to be investigated.

Author affiliations: [a]State Key Laboratory of Plant Environmental Resilience, College of Biological Sciences, Frontiers Science Center for Molecular Design Breeding (MOE), China Agricultural University, Beijing 100193, China; [b]Beijing Key Laboratory of Development and Quality Control of Ornamental Crops, Department of Ornamental Horticulture, College of Horticulture, China Agricultural University, Beijing 100193, China; [c]College of Life Sciences, Institute of Life Science and Green Development, Hebei University, Baoding 071002, China; and [d]Institute of Science and Technology Austria, Klosterneuburg 3400, Austria

Author contributions: J.Z. designed research; Y.W., Z.Y., J.W., H.X., L.W., and L.L. performed research; Y.W., Z.Y., L.L., Y.G., Z.G., J.F., and J.Z. analyzed data; and Y.W., Z.Y., J.F., and J.Z. wrote the paper.

The authors declare no competing interest.

This article is a PNAS Direct Submission.

[1]Y.W., Z.Y., and J.W. contributed equally to this work.

[2]To whom correspondence may be addressed. Email: zhangj@cau.edu.cn.

This article contains supporting information online at https://www.pnas.org/lookup/suppl/doi:10.1073/pnas.2221313120/-/DCSupplemental.

Published June 12, 2023.

The large NRT transporter family in Arabidopsis (*Arabidopsis thaliana*) comprises 53 NRT1 and seven NRT2 members (2). NRT1 family members appear to be critical for low-affinity NO_3^- transport (21), with the exception of NRT1.1, which not only acts as a dual-affinity NO_3^- transporter and NO_3^- sensor, but also functions in auxin translocation (1, 10–12). NRT2-type proteins have been characterized as specific high-affinity NO_3^- transporters, and to date, no other substrate has been identified (21, 22). The transporter activity of most NRT2 members depends on the partner protein nitrate assimilation–related protein (NAR2.1, also named NRT3.1), which is required for the plasma membrane targeting and protein stabilization of NRT2 members (21, 23). Among others, NRT2.1 serves as the predominant high-affinity NO_3^- transporter, as NO_3^- uptake capacity dropped by about 56% in *nrt2.1* knockouts (24). *NRT2.1* transcription is differentially regulated as a function of external NO_3^- levels. NO_3^- at low concentrations effectively induces *NRT2.1* expression, but higher concentrations repress it (25). Previous studies have reported a role for NRT2.1 in the response of lateral root initiation to low NO_3^- (26, 27). While NRT1.1 is known to use both NO_3^- and auxin as possible substrates to regulate lateral root development (1, 10), the mechanism by which NRT2.1 regulates root architecture is still unknown.

In this study, we used forward genetics to identify Arabidopsis *low-nitrate-resistant mutant2* (*lonr2*) whose primary root elongation showed reduced sensitivity to low NO_3^-. We discovered that *lonr2* mutants were defective in *NRT2.1*. *lonr2* (*nrt2.1*) mutants displayed impaired polar auxin transport and their low-NO_3^--induced root phenotype required auxin transport activity of PIN7. We established that NRT2.1 directly associated with PIN7 and antagonized PIN7-mediated auxin efflux in *Xenopus* (*Xenopus laevis*) oocytes and tobacco (*Nicotiana tabacum*) Bright Yellow-2 (BY-2) cells depending on NO_3^- levels. These observations extend the spectrum of biological function of NRT2.1, highlighting an important role in the adaptation of root growth to NO_3^- limitation by directly counteracting auxin transport activity.

Results

Identification of *lonr2* Mutants. Modulation of plant root architecture, including primary root growth, is an essential plant adaptive response to dynamically changing NO_3^- concentrations in the soil (28, 29). However, the molecular mechanisms underlying this adaptation remain largely unknown.

Different NO_3^- concentrations can either inhibit or stimulate primary root elongation (3, 5, 30–33). To further identify NO_3^--related regulators of root growth, we performed a forward genetic screen to look for Arabidopsis mutants that were less sensitive to low NO_3^- when grown on medium containing 0.05 mM NO_3^-. We identified three mutant lines, which we named *low-nitrate-resistant mutant2* (*lonr2-1* through *lonr2-3*). These lines harbored mutations that largely restored primary root growth under low-NO_3^- conditions (Fig. 1 *A* and *B*). We did not observe phenotypic differences between the roots of wild-type and *lonr2* seedlings when grown on 10 mM NO_3^- medium, but *lonr2* primary roots were much longer than those of wild-type seedlings when grown on 0.05 mM NO_3^- (Fig. 1 *A* and *B*). Genetic analysis indicated that the *lonr2-1* through *lonr2-3* mutations occur in a single gene (*SI Appendix*, Fig. S1 *A–D*).

Root length is coordinately determined by the activity of the root stem cell niche and the differentiation of the cell progenies.

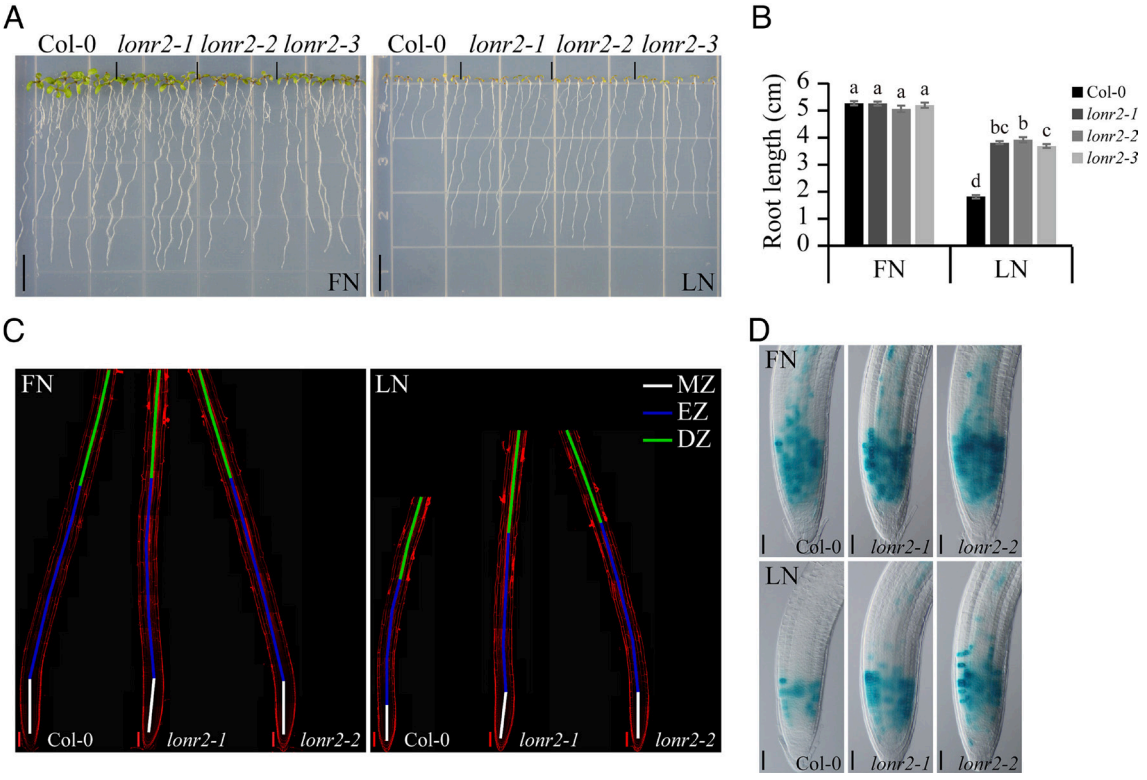

Fig. 1. *lonr2* mutants are less sensitive to low NO_3^- in terms of primary root elongation. (*A* and *B*) Root phenotypes (*A*) and primary root length (*B*) of *lonr2* mutants grown under 10 mM NO_3^- (full NO_3^-; FN) or 0.05 mM NO_3^- (low NO_3^-; LN) conditions for 9 to 10 d. (Scale bars, 1 cm.) Data are shown as means ± SE ($n \geq 17$ roots). Different lowercase letters indicate significant differences ($P < 0.05$; one-way ANOVA followed by Fisher's LSD test). (*C*) Confocal images of the root meristematic (white line), elongation (blue line), and differentiation (green line) zones of *lonr2* mutants. Each image is composed of several joined photographs of the same root. MZ, meristematic zone; EZ, elongation zone; DZ, differentiation zone. (Scale bars, 100 μm.) (*D*) Cell division activity in root meristems of *lonr2* mutants as visualized by *CYCB1;1:DB-GUS*. (Scale bars, 50 μm.)

Along the longitudinal axis of the root tip, cellular activities are separated spatially into the meristematic zone (MZ), elongation zone (EZ), and differentiation zone (DZ) (34, 35). To pinpoint the underlying cause of the altered growth of *lonr2* roots, we measured the cell numbers, cell lengths, and zone lengths of wild-type and *lonr2* roots grown at different NO_3^- concentrations. On medium with 10 mM NO_3^-, the lengths of the MZ, EZ, and DZ of *lonr2* seedlings were similar to those of wild-type seedlings; the seedlings had similar cell numbers and average cell lengths across the three zones (Fig. 1*C* and *SI Appendix*, Fig. S1*E*). Low-NO_3^- treatment decreased cell number and/or cell length in each zone to a greater extent in wild-type than in *lonr2* seedlings, leading to longer root zones in *lonr2* seedlings under low NO_3^- (Fig. 1*C* and *SI Appendix*, Fig. S1*E*). We also examined the expression of the mitotic marker *CYCB1;1:DB-GUS* in wild-type and *lonr2* seedlings. We observed a much higher cell division activity in *lonr2* root meristems than that in the wild type under low-NO_3^- conditions (Fig. 1*D*), suggesting that loss of LONR2 function promotes mitosis.

We next examined the effects of various concentrations of NO_3^- on root growth and determined that *lonr2* mutants had longer primary roots than those of wild-type seedlings when exposed to lower concentrations of NO_3^- (*SI Appendix*, Fig. S1*F*). However, there was no difference in root length between wild-type and *lonr2* seedlings at higher NO_3^- concentrations (*SI Appendix*, Fig. S1*F*). We also investigated the effect of ammonium (NH_4^+) on the root growth of *lonr2* mutants and observed that the mutants exhibited similar sensitivity as wild-type seedlings to all NH_4^+ concentrations tested (*SI Appendix*, Fig. S1*G*). Together, these results indicated that *LONR2* is involved in the regulation of root development, specifically under low-NO_3^- conditions.

***lonr2* Is Defective in the High-Affinity NO_3^- Transporter *NRT2.1*.** Using whole-genome sequencing, we identified the high-affinity NO_3^- transporter gene *NRT2.1* (At1g08090) as *LONR2*. One of the alleles introduced a premature stop codon (C to T at nucleotide 1405, R406STOP), and the other two alleles created different amino acid substitutions (G to A at nucleotide 247, A83T; G to A at nucleotide 592, G198S) (Fig. 2*A*). The T-DNA insertion mutant SALK_141712 (*nrt2.1* hereafter) had approximately 10% of the *NRT2.1* transcript level seen in the wild type (24) (*SI Appendix*, Fig. S2*A*). This mutant showed a phenotype similar to the other *lonr2* alleles grown on medium containing 0.05 mM NO_3^-; the roots of the *nrt2.1* mutant were much longer than those of the wild type (Fig. 2*B*). We next evaluated NO_3^- uptake and accumulation in the *lonr2* mutants. We observed that *lonr2-1* through *lonr2-3* seedlings exposed to $^{15}NO_3^-$ had significantly lower rates of NO_3^- influx compared to wild-type seedlings, as did the *nrt2.1* T-DNA insertion mutant (*SI Appendix*, Fig. S2*B*). Moreover, *lonr2-1* through *lonr2-3* alleles also had lower NO_3^- contents than wild type, resembling the *nrt2.1* T-DNA insertion mutant (*SI Appendix*, Fig. S2*C*). These results suggest that either the premature stop codon (R406STOP) or the altered amino acids (A83T, G198S) compromise the NRT2.1 function in NO_3^- uptake activity and thus reduce NO_3^- accumulation. Several previous studies have indicated that NRT2.1 has a regulatory role in the lateral root formation in response to NO_3^- limitation (26, 27). We therefore carefully analyzed lateral root initiation and development

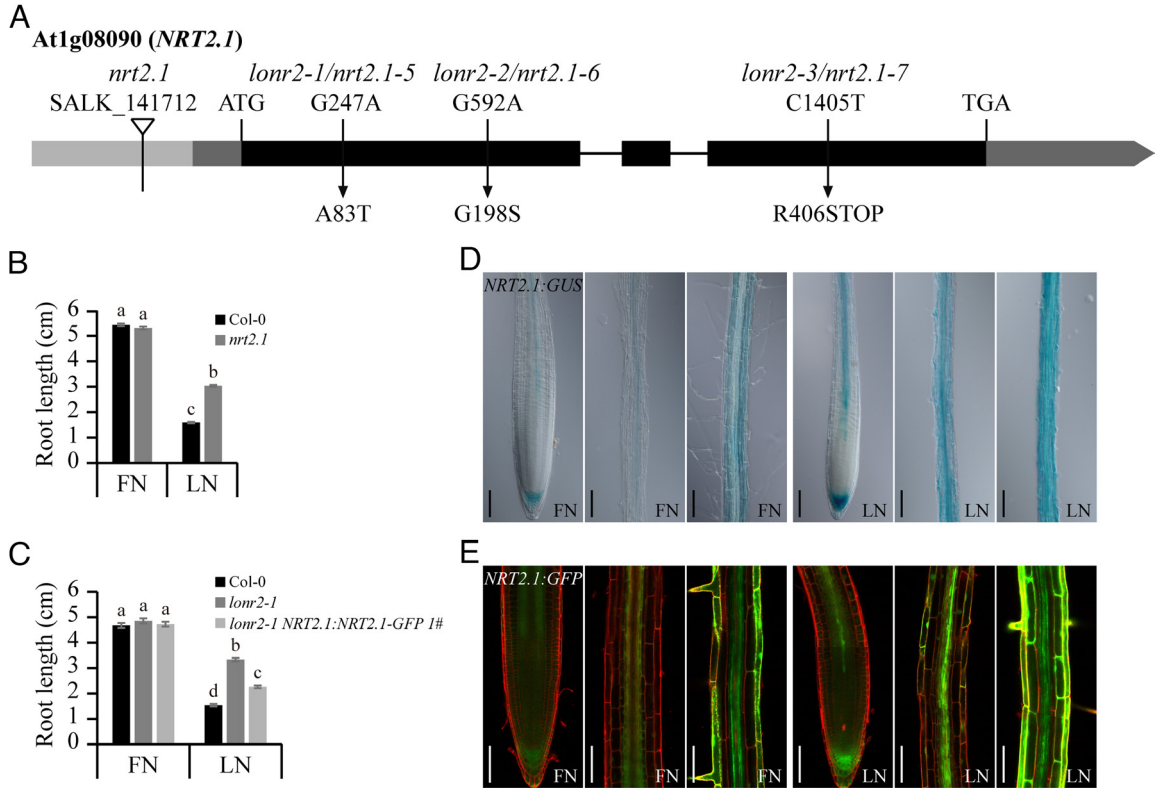

Fig. 2. *LONR2* encodes the NO_3^- transporter *NRT2.1*. (*A*) Genomic structure of the *LONR2/NRT2.1* mutant locus. Light gray box, promoter; dark gray boxes, UTRs; black boxes, exons; lines, introns. The relative positions of the *lonr2-1/nrt2.1-5, lonr2-2/nrt2.1-6*, and *lonr2-3/nrt2.1-7* mutations are indicated. T-DNA insertion for *nrt2.1* (SALK_141712) is 236 bp upstream of the start codon. (*B* and *C*) Primary root length of the T-DNA insertion mutant *nrt2.1* (*B*) and the *lonr2-1 NRT2.1:NRT2.1-GFP 1#* complementation line (*C*). Data are shown as means ± SE ($n \geq 20$ roots). Different lowercase letters indicate significant differences ($P < 0.05$; one-way ANOVA followed by Fisher's LSD test). (*D* and *E*) Expression pattern of the promoter fusions *NRT2.1:GUS* (*D*) and *NRT2.1:GFP* (*E*) in root meristematic, elongation, and differentiation zones (from *Left* to *Right*). Spatial patterns of GFP fluorescence are shown by two joined photographs of the same root. (Scale bars, 100 μm.)

in *lonr2* mutants under our experimental conditions and found that mutations identified in *lonr2-1* or *lonr2-2* did strongly reduce the density of lateral root primordia and emerged lateral roots under low-NO_3^- conditions (*SI Appendix*, Fig. S2*D*), which is consistent with the previous observations in other mutant alleles of *NRT2.1* (27). Thus, it is tempting to suggest that low-NO_3^--repressed root branching phenotype in *lonr2* was specifically due to *NRT2.1* mutation. The distinct growth behaviors of lateral roots and primary roots (i.e., an increase in root length) of *lonr2* mutants are likely caused by the different mechanisms or associated key regulators in response to exogenous cues.

We attempted to complement the *lonr2-1* allele with a C-terminal GFP fusion of *NRT2.1* under the control of its endogenous promoter (~1.9 kb). This transgene (*NRT2.1:NRT2.1-GFP*) only partially rescued the long root phenotype of *lonr2-1* under low-NO_3^- conditions (Fig. 2*C* and *SI Appendix*, Fig. S2*E*). We speculated that the partial rescue was likely due to impaired NRT2.1 function by the fused GFP. Therefore, we tested the previously reported transgenic line *nrt2.1 NRT2.1:NRT2.1* expressing the *NRT2.1* genomic fragment without GFP, which was shown to completely rescue the shoot growth–restricted phenotype of the *nrt2.1* T-DNA insertion allele (36). Importantly, even under the control of the shorter endogenous promoter (1.2 kb), the *NRT2.1:NRT2.1* transgene was able to fully complement the low-NO_3^--insensitive root growth phenotype of the *nrt2.1* mutant (*SI Appendix*, Fig. S2*F*).

Monitoring *NRT2.1* promoter activity in *NRT2.1:GUS* transgenic lines suggested that the gene has broad expression in cotyledons, floral organs (*SI Appendix*, Fig. S2*G*), and throughout the entire primary roots, including the MZ, EZ, and DZ (Fig. 2*D* and *SI Appendix*, Fig. S2*H*). In addition to epidermal and cortical cells, as previously reported (27, 37, 38), we also detected *NRT2.1* in the columella, lateral root caps, and vasculature of roots (Fig. 2*D* and *SI Appendix*, Fig. S2*H*). The same overall expression pattern in the roots was also detected in transgenic lines harboring an *NRT2.1:GFP* transgene (Fig. 2*E* and *SI Appendix*, Fig. S2*I*). In agreement with previous studies (25, 36), low NO_3^- promoted expression of *NRT2.1* as visualized by *NRT2.1:GUS* and *NRT2.1:GFP* (Fig. 2 *D* and *E* and *SI Appendix*, Fig. S2 *H* and *I*). These observations were further confirmed by reverse transcription-quantitative PCR (RT-qPCR) (*SI Appendix*, Fig. S2*J*).

The independent alleles and mutant complementation experiments above demonstrated that mutations in the *NRT2.1* gene are responsible for the low-NO_3^--hyposensitive root growth phenotype of *lonr2* mutants. Hence, we renamed the *lonr2-1*, *lonr2-2*, and *lonr2-3* mutants as *nrt2.1-5*, *nrt2.1-6*, and *nrt2.1-7*, respectively. *NRT2.1* encodes a major nitrogen starvation–inducible component of the NO_3^- high-affinity transport system (2, 25, 27). In addition to NO_3^- uptake, NRT2.1 also plays a crucial role in NO_3^- signaling, regulating lateral root initiation (26, 27). As such, NRT2.1 function would be required for root development, generally, with primary root elongation being only a subset of them.

***nrt2.1* Seedlings Are Defective in Auxin Transport.** Auxin is the main regulator of root system architecture (39, 40). To explore how NO_3^- regulates root development, we analyzed auxin accumulation in the *nrt2.1* alleles. We established that *nrt2.1* mutants always showed higher auxin signaling in their root tips under low-NO_3^- supply compared to wild-type seedlings, as visualized using the auxin response reporters *DR5rev:GFP* and DII-VENUS (Fig. 3 *A–D* and *SI Appendix*, Fig. S3 *A–D*). Consistent with these observations, the *nrt2.1* alleles grown on low NO_3^- had more endogenous indole-3-acetic acid (IAA) contents in their roots than those of wild-type seedlings (*SI Appendix*, Fig. S3*E*). These results indicate that NRT2.1 function leads to a reduction in auxin levels in root tips under low-NO_3^- conditions. The quantitative changes in auxin signaling activity and auxin contents thus suggested that NRT2.1 has a direct effect on auxin distribution.

Auxin accumulation at the root tip is the result of auxin biosynthesis and polar transport and determines auxin-mediated root growth (39, 41). We thus measured the expression levels of the auxin biosynthesis–related genes *tryptophan aminotransferase of Arabidopsis1* (42), *anthranilate synthase alpha subunit1* (43), and *AMIDASE1* (44) by RT-qPCR, and found that they were expressed at similar levels in wild-type and *nrt2.1* mutant seedlings grown under low-NO_3^- conditions (*SI Appendix*, Fig. S3*F*). Thus, these data suggest that *NRT2.1* may not regulate auxin biosynthesis. We next quantified auxin transport in the roots of *nrt2.1* mutants and observed higher acropetal (toward the root tip) IAA transport under low-NO_3^- conditions compared to that in the wild type (Fig. 3*E*). This result is consistent with the low-NO_3^--induced auxin response and auxin levels in roots of *nrt2.1* mutants (Fig. 3 *A–D* and *SI Appendix*, Fig. S3 *A–E*). In summary, *nrt2.1* loss-of-function phenotypes hint at a role for NRT2.1 in NO_3^--regulated root development, presumably as a result of the misregulated auxin transport.

Directional cell-to-cell auxin transport is mediated by, among other proteins, members of the canonical PIN auxin exporter family, which exhibit polar localization at the plasma membrane (41, 45, 46). To investigate the genetic interaction between NRT2.1 and PIN proteins, we crossed the *nrt2.1* T-DNA insertion mutant with various *pin* loss-of-function mutants. The *pin* mutants displayed tolerance to low NO_3^- comparable to that of wild-type seedlings (Fig. 3*F* and *SI Appendix*, Fig. S3 *G–I*). Under low-NO_3^- conditions, the double mutants *nrt2.1 eir1-1*, *nrt2.1 pin3-4*, and *nrt2.1 pin4-3* had the same enhanced root elongation as the *nrt2.1* single mutant (*SI Appendix*, Fig. S3 *G–I*). By contrast, *pin7-2* substantially suppressed the lower sensitivity to low NO_3^- of *nrt2.1* in terms of root elongation (Fig. 3*F*). Moreover, under 0.05 mM NO_3^- conditions, *pin7-2* also restored the normal endogenous IAA levels and acropetal IAA transport in *nrt2.1* roots, as inferred from direct measurements of IAA contents and ^{3}H-IAA accumulation (Fig. 3*G* and *SI Appendix*, Fig. S3*J*). Thus, we conclude that *pin7* suppresses various aspects of the *nrt2.1* phenotype.

We also generated transgenic plants carrying the *Super:PIN7-Flag* transgene in the wild-type background. Overexpressing *PIN7* caused a low-NO_3^--hyposensitive phenotype affecting root elongation (Fig. 3*H*), similar to that of the *nrt2.1* mutants. To further explore the genetic interaction between NRT2.1 and PIN7, we crossed *Super:PIN7-Flag* with *Super:NRT2.1-Flag*. In the F1 generation, we observed that *NRT2.1* overexpression fully blocked the long-root phenotype of the *PIN7* gain-of-function line when grown on medium containing 0.05 mM NO_3^- (Fig. 3*I*). Moreover, transgenic seedlings stably overexpressing *PIN7* in the *nrt2.1* mutant background were even more resistant than *nrt2.1* mutants to low NO_3^- in terms of root growth (Fig. 3*J*). Collectively, these results reveal that the auxin efflux carrier PIN7 acts specifically downstream of NRT2.1 to positively regulate root growth in response to low-NO_3^- availability.

NRT2.1 Interacts Directly with PIN7 and Interferes with PIN7 Auxin Transport Activity. *NRT2.1* and *PIN7* are expressed in largely overlapping patterns in columella and stele cells of the roots (47), and both are NO_3^--regulated genes (25, 38) (Fig. 2 *D* and *E* and *SI Appendix*, Figs. S2 *H* and *I* and S4 *A* and *B*). Low concentration of NO_3^- is most effective in promoting NRT2.1,

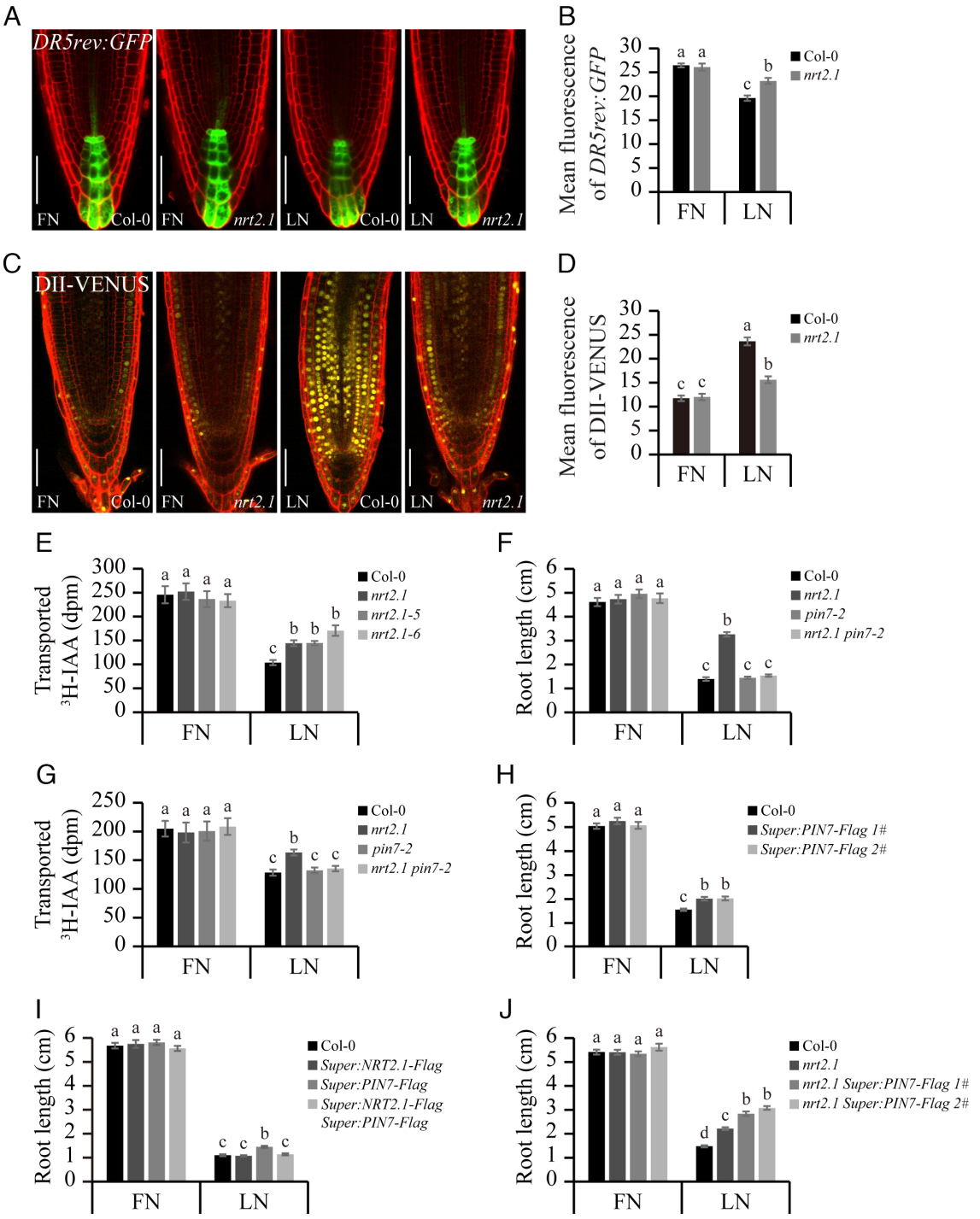

Fig. 3. *nrt2.1* is defective in auxin transport. (*A*–*D*) Effects of low NO_3^- on auxin signaling in the root tips of the *nrt2.1* T-DNA insertion mutant as revealed by expression analysis of *DR5rev:GFP* and DII-VENUS. The fluorescence intensity of *DR5rev:GFP* (*A*) and DII-VENUS (*C*) reporters is quantified in (*B*) and (*D*), respectively. (Scale bars, 50 μm.) Data are shown as means ± SE ($n \geq 15$ roots). Different lowercase letters indicate significant differences ($P < 0.05$; one-way ANOVA followed by Fisher's LSD test). (*E*) Measurements of acropetal auxin transport in roots of *nrt2.1* mutants. Data are shown as means ± SE ($n \geq 14$ roots). Different lowercase letters indicate significant differences ($P < 0.05$; one-way ANOVA followed by Fisher's LSD test). (*F*) Primary root length in the *nrt2.1 pin7-2* double mutant. Data are shown as means ± SE ($n \geq 18$ roots). Different lowercase letters indicate significant differences ($P < 0.05$; one-way ANOVA followed by Fisher's LSD test). (*G*) Measurements of acropetal auxin transport in roots of the *nrt2.1 pin7-2* double mutant. Data are shown as means ± SE ($n \geq 16$ roots). Different lowercase letters indicate significant differences ($P < 0.05$; one-way ANOVA followed by Fisher's LSD test). (*H*–*J*) Primary root length in *Super:PIN7-Flag* seedlings (*H*), the F1 progeny from a cross between *Super:NRT2.1-Flag* and *Super:PIN7-Flag* seedlings (*I*), and *nrt2.1 Super:PIN7-Flag* lines (*J*). Data are shown as means ± SE ($n \geq 14$ roots). Different lowercase letters indicate significant differences ($P < 0.05$; one-way ANOVA followed by Fisher's LSD test).

but inhibiting PIN7 expression (Fig. 2 *D* and *E* and *SI Appendix*, Figs. S2 *H* and *I* and S4*B*).

We next assessed PIN7 expression pattern in the *nrt2.1-6* mutant background. Notably, *NRT2.1* mutation did not visibly affect PIN7 localization, reflected by the preferential occurrence of PIN7 at the basal side of stele cells and nonpolar plasma membrane distribution in the columella cells (48) (*SI Appendix*, Fig. S4*C*). Meanwhile, we also noticed no change of *PIN7:PIN7-GFP* signal intensity in *nrt2.1-6* in response to NO_3^- availability when compared to that in the wild-type roots (*SI Appendix*,

Fig. S4 *C* and *D*). Hence, these results suggest that NRT2.1 does not modulate PIN7 expression.

Considering that NRT2.1 and PIN7 are plasma membrane–localized transporters (2, 47), we next wondered whether NRT2.1 may directly interact with PIN7. To this end, we conducted yeast two-hybrid (Y2H) assays by cotransforming constructs encoding the N-terminal domain of NRT2.1 fused to the yeast GAL4 activation domain (*AD-NRT2.1N*) and the PIN7 hydrophilic loop fused with the GAL4 DNA-binding domain (*BD-PIN7HL*) into yeast strain AH109. We observed that NRT2.1N directly interacted with PIN7HL in yeast cells (Fig. 4*A*). We also performed coimmunoprecipitation (Co-IP) assays using total proteins extracted from Arabidopsis wild-type protoplasts transiently expressing *NRT2.1N-GFP* and *PIN7HL-Flag* constructs. We established that NRT2.1N coimmunoprecipitated with PIN7HL in vivo (Fig. 4*B*). The interaction between NRT2.1N and PIN7HL was further confirmed using a luciferase complementation imaging (LCI) assay by *Agrobacterium tumefaciens*–mediated transient coexpression in *Nicotiana benthamiana* leaves (*SI Appendix*, Fig. S4 *E-G*). Notably, the interaction of NRT2.1N and PIN7HL was attenuated by spraying the leaves with 10 mM NO_3^- (Fig. 4 *C* and *D*). These observations reveal that NRT2.1 physically interacts with PIN7 in vitro and in vivo, and that this interaction is sensitive to NO_3^-.

To investigate the physiological relevance of NRT2.1 and the NRT2.1–PIN7 interaction in NO_3^--regulated root development, we measured the auxin transport activity of NRT2.1 in a heterologous test system using *Xenopus* oocytes. As reported previously (22, 38), bimolecular fluorescence complementation signal for the interaction between full-length NRT2.1 and NRT3.1 was detected at the plasma membrane of the oocytes (*SI Appendix*, Fig. S5*A*). The proper accumulation of PIN7 at the plasma membrane in oocytes was also confirmed by immunoblot analysis (*SI Appendix*, Fig. S5*B*). Consistent with a previous study (49), we observed that the oocytes coexpressing PIN7 and serine/threonine protein kinase PINOID (PID) accumulated less ^{3}H-IAA than that of the background control (Fig. 4*E*). Auxin efflux in oocytes coexpressing NRT2.1 and NRT3.1 did not differ from that in the background control, suggesting that NRT2.1 cannot directly transport auxin. However, when we coinjected complementary RNA (cRNA) of NRT2.1 and NRT3.1 with PIN7 and PID into oocytes, we measured significantly higher ^{3}H-IAA accumulation compared to that in oocytes expressing PIN7 and PID only (Fig. 4*E*). Because PID was coexpressed with NRT2.1 in these experiments, it is unclear whether the differences in intracellular auxin accumulation observed in oocytes are a result of modulated NRT2.1 activity by PID kinase through direct phosphorylation. Hence, we first investigated the possibility of physical interaction between PID and NRT2.1. By preforming Y2H and Co-IP assays, we observed that PID did not associate with NRT2.1N in vitro and in vivo (*SI Appendix*, Fig. S5 *C* and *D*). To establish whether PID kinase could phosphorylate NRT2.1, we next performed in vitro phosphorylation assays with recombinant proteins. Although we demonstrated that PID underwent autophosphorylation and mediated the phosphorylation of PIN2HL, no phosphorylated band of NRT2.1N was observed (*SI Appendix*, Fig. S5*E*). Moreover, we coinjected cRNA of NRT2.1 and NRT3.1 with PID into oocytes, and we observed that the amount of NO_3^- retained was essentially unchanged compared to that in oocytes expressing NRT2.1 and NRT3.1 (*SI Appendix*, Fig. S5*F*), indicating that NO_3^- uptake activity of NRT2.1 is not dependent on PID kinase. We also tested the potential PID effect on NRT2.1 in ^{3}H-IAA efflux assays and found that NRT2.1 alone or NRT2.1 and NRT3.1 together could not directly transport auxin regardless of the presence or absence of PID (Fig. 4*E*). Together, these observations exclude the involvement of PID in regulating NRT2.1 activity. Furthermore, to rule out the possibility of artifacts induced by overloading oocytes with multiple samples, we also included several negative controls among the transport assays. Importantly, we observed that PIN7-mediated ^{3}H-IAA efflux was not influenced by the NRT2.1^{R406STOP} variant (the mutation identified in *lonr2-3*) with impaired NO_3^- uptake (*SI Appendix*, Fig. S5*F*), the plasma membrane intrinsic protein PIP2;1, or the NO_3^- transporter NRT2.5 (Fig. 4*E* and *SI Appendix*, Fig. S5*G*). In summary, these data show that although NRT2.1 is not an auxin transporter, it specifically antagonizes PIN7-mediated auxin efflux in the oocyte expression system.

Tobacco BY-2 suspension cells provide a well-established and tractable model for measuring auxin transport. Therefore, we determined the effect of NRT2.1 on auxin transport activity of PIN7 in BY-2 cells. First, we verified the normal expression levels of *NRT2.1* and *PIN7* in BY-2 cell lines by RT-qPCR (*SI Appendix*, Fig. S5*H*). Without NO_3^- treatment, cells stably expressing PIN7 accumulated less ^{3}H-IAA than that of control cells transfected with the empty vector (Fig. 4*F*). Coexpression of NRT2.1 and NRT3.1 had no effect on ^{3}H-IAA accumulation but clearly interfered with PIN7-mediated auxin efflux (Fig. 4*F*). In agreement with the oocyte data, when NRT2.1 was replaced with the truncated variant NRT2.1^{R406STOP}, or the plasma membrane–localized PIP2;1, or the NO_3^- transporter NRT2.5, PIN7-dependent auxin transport was no longer influenced (Fig. 4*F*). However, when BY-2 cells were treated with NO_3^- (5 mM), PIN7-mediated IAA efflux was no longer affected by the presence of NRT2.1 (Fig. 4*F*). This observation is consistent with the *nrt2.1* defects specifically seen under low-NO_3^- conditions (*SI Appendix*, Fig. S1*F*). To further determine whether the effect on auxin transport is due to indirect factors associated with low-NO_3^- conditions, we measured ATP levels and apoplastic pH in BY-2 cells under different external NO_3^- concentrations. Notably, changes in NO_3^- availability did not affect either the ATP concentration or the apoplastic pH (*SI Appendix*, Fig. S5 *I* and *J*). Together, these results suggest that NRT2.1 negatively and specifically affects PIN7-induced auxin transport in BY-2 cells, and this regulation is dependent on NO_3^- levels.

Taken together, these data suggest that the high-affinity NO_3^- transporter NRT2.1, which responds to NO_3^- availability, specifically interferes with PIN7-mediated auxin transport under limited NO_3^- conditions and thereby regulates root growth.

Discussion

Modulation of primary root growth is a prominent foraging strategy for adaptation to NO_3^- fluctuation (28, 29); however, the underlying molecular mechanisms remain to be investigated. In this study, we identified *lonr2* mutants with a defect in low-NO_3^--mediated suppression of primary root growth. We determined that *LONR2* was the previously characterized high-affinity NO_3^- transporter gene *NRT2.1*. Our results indicated that *LONR2/NRT2.1* plays an essential role in regulating primary root elongation in response to low-NO_3^- stress. We uncovered a functional interaction between NRT2.1 and PIN7, finding that NRT2.1 interfered with PIN7-mediated auxin efflux under low-NO_3^- conditions (Fig. 5). This study reveals a previously unanticipated mechanism behind adaptive root development.

Although NO_3^- uptake rates are compromised in *nrt2.1* mutants (24, 26, 27) (*SI Appendix*, Fig. S2*B*), our results support the idea that the loss of NRT2.1 function promotes primary root elongation under low-NO_3^- conditions independently of this reduced

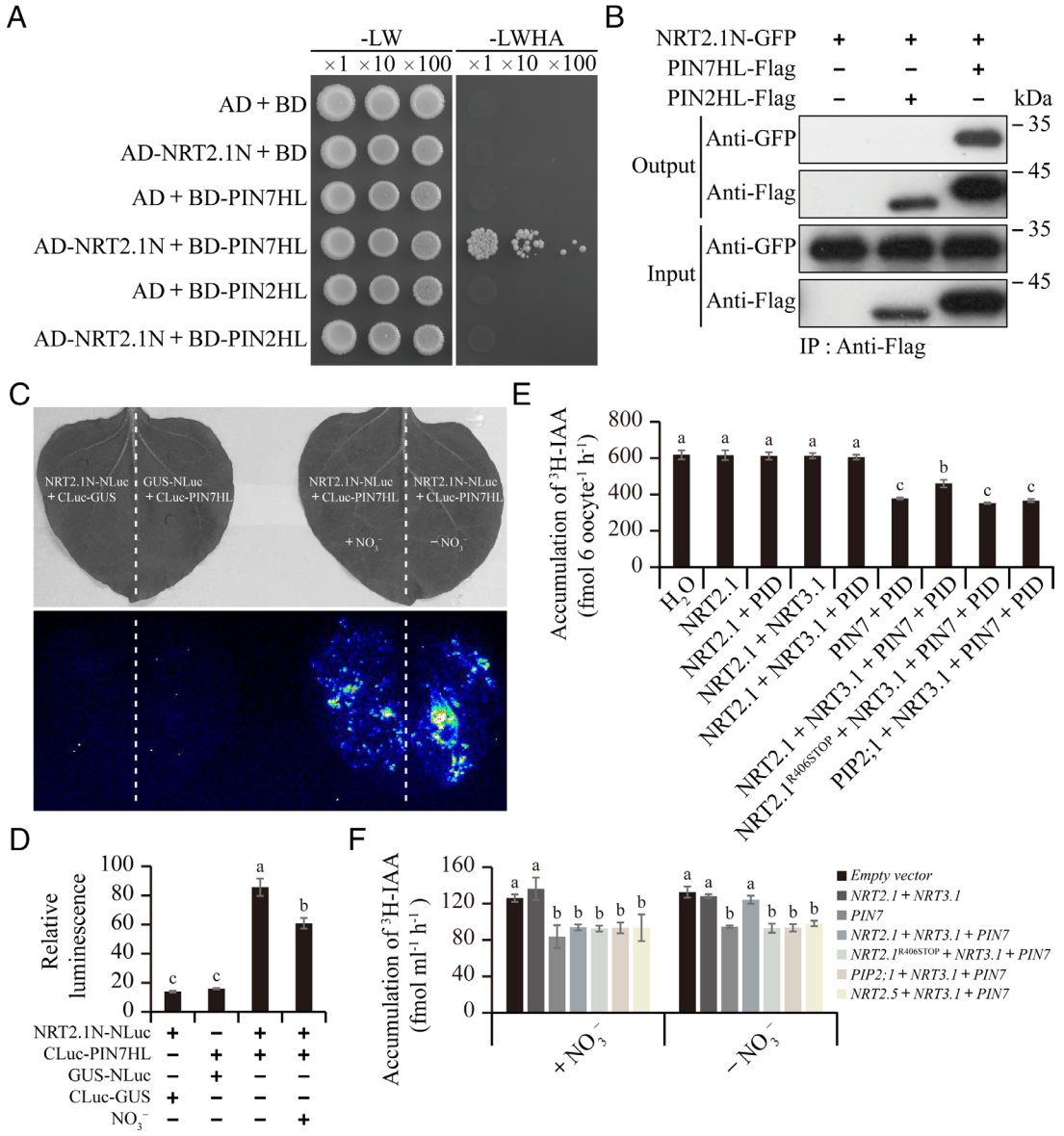

Fig. 4. NRT2.1 physically interacts with PIN7 and interferes with PIN7-mediated auxin transport activity. (*A*) Y2H assay demonstrating that NRT2.1N interacts with PIN7HL. As a negative control, NRT2.1N does not interact with PIN2HL. -LW, synthetic defined (SD) medium lacking Leu and Trp; -LWHA, SD medium lacking Leu, Trp, His, and Ade. (*B*) Co-IP assay demonstrating that NRT2.1N interacts with PIN7HL in Arabidopsis protoplasts. As a negative control, NRT2.1N does not coimmunoprecipitate with PIN2HL. (*C* and *D*) LCI assay demonstrating that interaction between NRT2.1N and PIN7HL is attenuated by application of 10 mM NO_3^- in *N. benthamiana* leaves. The luciferase signal intensity (*C*) is quantified in (*D*). Data are shown as means ± SE ($n = 24$ replicates). Different lowercase letters indicate significant differences ($P < 0.05$; one-way ANOVA followed by Fisher's LSD test). (*E*) Auxin efflux assays in *Xenopus* oocytes injected with different cRNAs as specified. Data are shown as means ± SE ($n = 4$ replicates; each replicate contains six oocytes). Different lowercase letters indicate significant differences ($P < 0.05$; one-way ANOVA followed by Fisher's LSD test). (*F*) Auxin efflux assays in BY-2 cells expressing the indicated constructs under different external NO_3^- conditions. Data are shown as means ± SE ($n \geq 3$ replicates; each replicate contains 0.5 mL suspension cells). Different lowercase letters indicate significant differences ($P < 0.05$; one-way ANOVA followed by Fisher's LSD test).

NO_3^- uptake. When NO_3^- was almost depleted from the medium, wild-type seedlings did not recapitulate the phenotype of *nrt2.1* mutants (*SI Appendix*, Fig. S1*F*). Conversely, when exogenous NO_3^- concentrations gradually increased, root growth of *nrt2.1* mutants was not repressed (*SI Appendix*, Fig. S1*F*). Therefore, we propose that NRT2.1 plays a role in developmental signaling in addition to its function in high-affinity NO_3^- uptake.

Due to its role in NO_3^- uptake, we expected *NRT2.1* expression to be confined to the outer cell layers of mature roots (27, 37, 38), as this is where the bulk of nutrient uptake usually occurs. However, according to our observations of promoter and functional fusions in this study, *NRT2.1* was expressed throughout the entire root. Indeed, we detected NRT2.1 in the columella, lateral root caps, epidermis, cortex, and vasculature of roots (Fig. 2 *D* and *E* and *SI Appendix*, Figs. S2 *H* and *I* and S4*A*). The discrepancy between previous studies and our results likely reflects the use of shorter *NRT2.1* promoter fragments in the previous reports (27, 37, 38). Although unexpected at first glance, this widespread expression pattern in roots hints that NRT2.1 must have a second function in addition to its role in NO_3^- uptake. The overlapping expression patterns of NRT2.1 and the auxin efflux carriers (e.g., PIN7) in root columella and vascular cells raise the possibility that these proteins have at least partially overlapping functions, which are probably related to auxin transport.

As demonstrated by the Y2H, Co-IP, and LCI assays, NRT2.1 physically interacted with PIN7 (Fig. 4 *A* and *B* and *SI Appendix*,

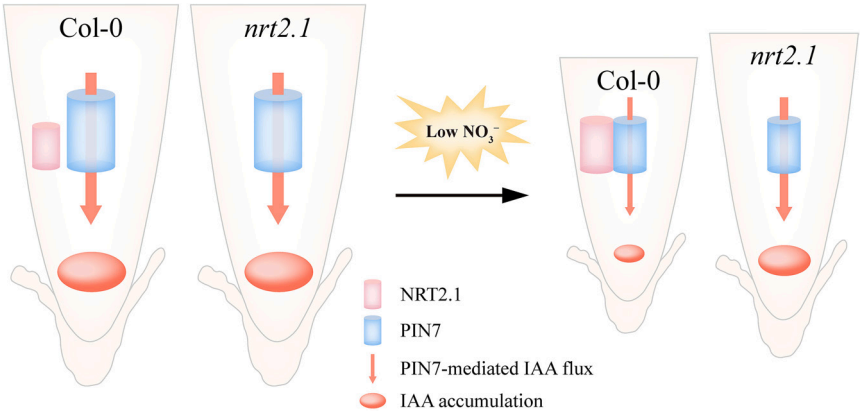

Fig. 5. Schematic conceptual model for NRT2.1 control of primary root growth in response to NO_3^- availability. Two situations are shown to illustrate the specific effect of low NO_3^- on primary root growth of the wild type and the *nrt2.1* mutant. The model postulates that under NO_3^--limited conditions, expression of the high-affinity NO_3^- transporter *NRT2.1* is induced and accumulated NRT2.1 directly interacts with the auxin efflux carrier PIN7, which in turn suppresses PIN7-mediated acropetal auxin efflux. This ultimately slows down primary root elongation. Conversely, lack of *NRT2.1* relieves auxin export activity of PIN7, eventually facilitating the rootward polar auxin transport by PIN7 and accelerating adaptive root growth in response to low NO_3^-.

Fig. S4 *E*–*G*). Unlike NRT1.1, which directly transports auxin, NRT2.1 did not; instead, we showed that it antagonized the auxin efflux activity of PIN7 in *Xenopus* oocytes and tobacco BY-2 cells depending on NO_3^- levels (Fig. 4 *E* and *F*). Given that auxin is structurally similar to one of the important nitrogen source amino acids, such as tryptophan (50, 51), it is not surprising that the NO_3^- transporter NRT2.1 might also participate in auxin transport. Indeed, several lines of evidence support the notion that NRT1.1 also directly transports auxin (1). Here, the observations that NRT2.1 expression inhibits PIN7-mediated auxin efflux in oocytes or BY-2 cells whereas the mutated variant $NRT2.1^{R406STOP}$, the plasma membrane–localized PIP2;1, or the NO_3^- transporter NRT2.5 did not (Fig. 4 *E* and *F* and *SI Appendix*, Fig. S5*G*), rule out the possibility of artifacts caused by the heterologous expression of transporters. The elevated acropetal auxin transport seen in *nrt2.1* mutants was clearly suppressed in the *nrt2.1 pin7-2* double mutant (Fig. 3*G*), confirming the idea that NRT2.1 regulates auxin transport *in planta*. Thus, in this study, we established a regulatory mechanism, whereby NRT2.1 plays a critical role in the integration of environmental and physiological information in response to nutrient availability. However, further research is needed to determine whether other factors contribute to the interaction between NRT2.1 and PIN7 and whether this interaction is regulated by protein modification events, such as phosphorylation.

In summary, we demonstrated that NRT2.1 modulates root growth in response to fluctuating NO_3^- availability in the soil, interacts with PIN7, and interferes with PIN7-mediated auxin transport activity depending on NO_3^- levels. Manipulation of the evolutionarily conserved gene *NRT2.1* (52, 53) may enable targeted engineering of auxin flux to achieve desired changes in root architecture and development, especially in food crops.

Materials and Methods

Plant Materials and Growth Conditions. The following previously described mutant and transgenic Arabidopsis plants were used: *nrt2.1* (SALK_141712) (24); *nrt2.1 NRT2.1:NRT2.1* (36); *eir1-1* (54); *pin4-3* (55); *pin3-4*, *pin7-2*, and *DR5rev:GFP* (56); DII-VENUS (57); *CYCB1;1:DB-GUS* (58); and *PIN7:PIN7-GFP* (59). The primers used for genotyping are listed in *SI Appendix*, Table S1.

Arabidopsis seedlings were grown on full-strength NO_3^- (10 mM) and low-NO_3^- medium (0.05 mM) as described (9). Arabidopsis ecotype Columbia (Col-0) was used as the wild type in this study.

Detailed *Materials and Methods* can be found in *SI Appendix*.

Data, Materials, and Software Availability. All study data are included in the article and/or *SI Appendix*.

ACKNOWLEDGMENTS. We are grateful to Caifu Jiang for providing ethyl methanesulfonate-mutagenized population, Yi Wang for providing *Xenopus* oocytes, Jun Fan and Zhaosheng Kong for providing tobacco BY-2 cells, and Claus Schwechheimer, Alain Gojon, and Shutang Tan for helpful discussions. This work was supported by the National Key Research and Development Program of China (2021YFF1000500), the National Natural Science Foundation of China (32170265 and 32022007), Hainan Provincial Natural Science Foundation of China (323CXTD379), Chinese Universities Scientific Fund (2023TC019), Beijing Municipal Natural Science Foundation (5192011), Beijing Outstanding University Discipline Program, and China Postdoctoral Science Foundation (BH2020259460).

1. G. Krouk *et al.*, Nitrate-regulated auxin transport by NRT1.1 defines a mechanism for nutrient sensing in plants. *Dev. Cell* **18**, 927–937 (2010).
2. J. A. O'Brien *et al.*, Nitrate transport, sensing, and responses in plants. *Mol. Plant* **9**, 837–856 (2016).
3. K. H. Liu *et al.*, Discovery of nitrate-CPK-NLP signalling in central nutrient-growth networks. *Nature* **545**, 311–316 (2017).
4. A. Gaudinier *et al.*, Transcriptional regulation of nitrogen-associated metabolism and growth. *Nature* **563**, 259–264 (2018).
5. T. Araya *et al.*, CLE-CLAVATA1 peptide-receptor signaling module regulates the expansion of plant root systems in a nitrogen-dependent manner. *Proc. Natl. Acad. Sci. U.S.A.* **111**, 2029–2034 (2014).
6. R. Tabata *et al.*, Perception of root-derived peptides by shoot LRR-RKs mediates systemic N-demand signaling. *Science* **346**, 343–346 (2014).
7. Y. Ohkubo, M. Tanaka, R. Tabata, M. Ogawa-Ohnishi, Y. Matsubayashi, Shoot-to-root mobile polypeptides involved in systemic regulation of nitrogen acquisition. *Nat. Plants* **3**, 17029 (2017).
8. Z. Jia, R. F. H. Giehl, R. C. Meyer, T. Altmann, N. von Wirén, Natural variation of BSK3 tunes brassinosteroid signaling to regulate root foraging under low nitrogen. *Nat. Commun.* **10**, 2378 (2019).
9. Y. Wang, Z. Gong, J. Friml, J. Zhang, Nitrate modulates the differentiation of root distal stem cells. *Plant Physiol.* **180**, 22–25 (2019).
10. X. Zhang *et al.*, Phosphorylation-mediated dynamics of nitrate transceptor NRT1.1 regulate auxin flux and nitrate signaling in lateral root growth. *Plant Physiol.* **181**, 480–498 (2019).
11. K. H. Liu, Y. F. Tsay, Switching between the two action modes of the dual-affinity nitrate transporter CHL1 by phosphorylation. *EMBO J.* **22**, 1005–1013 (2003).
12. C. H. Ho, S. H. Lin, H. C. Hu, Y. F. Tsay, CHL1 functions as a nitrate sensor in plants. *Cell* **138**, 1184–1194 (2009).
13. X. Sun *et al.*, Low nitrogen induces root elongation via auxin-induced acid growth and auxin-regulated target of rapamycin (TOR) pathway in maize. *J. Plant Physiol.* **254**, 153281 (2020).
14. R. A. Gutiérrez *et al.*, Qualitative network models and genome-wide expression data define carbon/nitrogen-responsive molecular machines in Arabidopsis. *Genome Biol.* **8**, R7 (2007).

15. K. Ötvös *et al.*, Modulation of plant root growth by nitrogen source-defined regulation of polar auxin transport. *EMBO J.* **40**, e106862 (2021).
16. M. L. Gifford, A. Dean, R. A. Gutierrez, G. M. Coruzzi, K. D. Birnbaum, Cell-specific nitrogen responses mediate developmental plasticity. *Proc. Natl. Acad. Sci. U.S.A.* **105**, 803–808 (2008).
17. E. A. Vidal *et al.*, Nitrate-responsive miR393/AFB3 regulatory module controls root system architecture in *Arabidopsis thaliana*. *Proc. Natl. Acad. Sci. U.S.A.* **107**, 4477–4482 (2010).
18. E. A. Vidal, T. C. Moyano, E. Riveras, O. Contreras-López, R. A. Gutiérrez, Systems approaches map regulatory networks downstream of the auxin receptor AFB3 in the nitrate response of *Arabidopsis thaliana* roots. *Proc. Natl. Acad. Sci. U.S.A.* **110**, 12840–12845 (2013).
19. L. H. Yu *et al.*, MADS-box transcription factor AGL21 regulates lateral root development and responds to multiple external and physiological signals. *Mol. Plant* **7**, 1653–1669 (2014).
20. T. T. Zhang *et al.*, NIN-like protein 7 promotes nitrate-mediated lateral root development by activating transcription of TRYPTOPHAN AMINOTRANSFERASE RELATED 2. *Plant Sci.* **303**, 110771 (2021).
21. Y. Y. Wang, Y. H. Cheng, K. E. Chen, Y. F. Tsay, Nitrate transport, signaling, and use efficiency. *Annu. Rev. Plant Biol.* **69**, 85–122 (2018).
22. M. Orsel *et al.*, Characterization of a two-component high-affinity nitrate uptake system in Arabidopsis. Physiology and protein-protein interaction. *Plant Physiol.* **142**, 1304–1317 (2006).
23. Z. Kotur *et al.*, Nitrate transport capacity of the *Arabidopsis thaliana* NRT2 family members and their interactions with AtNAR2.1. *New Phytol.* **194**, 724–731 (2012).
24. W. Li *et al.*, Dissection of the AtNRT2.1: AtNRT2.2 inducible high-affinity nitrate transporter gene cluster. *Plant Physiol.* **143**, 425–433 (2007).
25. T. Girin *et al.*, Identification of Arabidopsis mutants impaired in the systemic regulation of root nitrate uptake by the nitrogen status of the plant. *Plant Physiol.* **153**, 1250–1260 (2010).
26. D. Y. Little *et al.*, The putative high-affinity nitrate transporter NRT2.1 represses lateral root initiation in response to nutritional cues. *Proc. Natl. Acad. Sci. U.S.A.* **102**, 13693–13698 (2005).
27. T. Remans *et al.*, A central role for the nitrate transporter NRT2.1 in the integrated morphological and physiological responses of the root system to nitrogen limitation in Arabidopsis. *Plant Physiol.* **140**, 909–921 (2006).
28. J. López-Bucio, A. Cruz-Ramírez, L. Herrera-Estrella, The role of nutrient availability in regulating root architecture. *Curr. Opin. Plant Biol.* **6**, 280–287 (2003).
29. M. L. Gifford *et al.*, Plasticity regulators modulate specific root traits in discrete nitrogen environments. *PLoS Genet.* **9**, e1003760 (2013).
30. L. C. Chu *et al.*, Plasma membrane calcineurin B-like calcium-ion sensor proteins function in regulating primary root growth and nitrate uptake by affecting global phosphorylation patterns and microdomain protein distribution. *New Phytol.* **229**, 2223–2237 (2021).
31. Q. Ma, R. J. Tang, X. J. Zheng, S. M. Wang, S. Luan, The calcium sensor CBL7 modulates plant responses to low nitrate in Arabidopsis. *Biochem. Biophys. Res. Commun.* **468**, 59–65 (2015).
32. P. A. Naulin *et al.*, Nitrate induction of primary root growth requires cytokinin signaling in *Arabidopsis thaliana*. *Plant Cell Physiol.* **61**, 342–352 (2020).
33. X. Song *et al.*, CALMODULIN-LIKE-38 and PEP1 RECEPTOR 2 integrate nitrate and brassinosteroid signals to regulate root growth. *Plant Physiol.* **187**, 1779–1794 (2021).
34. L. Moubayidin *et al.*, Spatial coordination between stem cell activity and cell differentiation in the root meristem. *Dev. Cell* **26**, 405–415 (2013).
35. A. P. Fisher, R. Sozzani, Uncovering the networks involved in stem cell maintenance and asymmetric cell division in the Arabidopsis root. *Curr. Opin. Plant Biol.* **29**, 38–43 (2016).
36. X. Zou, M. Y. Liu, W. H. Wu, Y. Wang, Phosphorylation at Ser28 stabilizes the Arabidopsis nitrate transporter NRT2.1 in response to nitrate limitation. *J. Integr. Plant Biol.* **62**, 865–876 (2020).
37. P. Nazoa *et al.*, Regulation of the nitrate transporter gene AtNRT2.1 in *Arabidopsis thaliana*: responses to nitrate, amino acids and developmental stage. *Plant Mol. Biol.* **52**, 689–703 (2003).
38. J. Wirth *et al.*, Regulation of root nitrate uptake at the NRT2.1 protein level in *Arabidopsis thaliana*. *J. Biol. Chem.* **282**, 23541–23552 (2007).
39. J. Friml, Fourteen stations of auxin. *Cold Spring Harb. Perspect. Biol.* **14**, a039859 (2022).
40. G. Xiao, Y. Zhang, Adaptive growth: shaping auxin-mediated root system architecture. *Trends Plant Sci.* **25**, 121–123 (2020).
41. M. Adamowski, J. Friml, PIN-dependent auxin transport: action, regulation, and evolution. *Plant Cell* **27**, 20–32 (2015).
42. A. N. Stepanova *et al.*, TAA1-mediated auxin biosynthesis is essential for hormone crosstalk and plant development. *Cell* **133**, 177–191 (2008).
43. A. N. Stepanova, J. M. Hoyt, A. A. Hamilton, J. M. Alonso, A Link between ethylene and auxin uncovered by the characterization of two root-specific ethylene-insensitive mutants in Arabidopsis. *Plant Cell* **17**, 2230–2242 (2005).
44. Y. Mano *et al.*, The AMI1 gene family: indole-3-acetamide hydrolase functions in auxin biosynthesis in plants. *J. Exp. Bot.* **61**, 25–32 (2010).
45. M. Sauer, J. Kleine-Vehn, PIN-FORMED and PIN-LIKES auxin transport facilitators. *Development* **146**, dev168088 (2019).
46. L. R. Band, Auxin fluxes through plasmodesmata. *New Phytol.* **231**, 1686–1692 (2021).
47. A. Vieten *et al.*, Functional redundancy of PIN proteins is accompanied by auxin-dependent cross-regulation of PIN expression. *Development* **132**, 4521–4531 (2005).
48. E. Feraru, J. Friml, PIN polar targeting. *Plant Physiol.* **147**, 1553–1559 (2008).
49. M. Zourelidou *et al.*, Auxin efflux by PIN-FORMED proteins is activated by two different protein kinases, D6 PROTEIN KINASE and PINOID. *Elife* **3**, e02860 (2014).
50. L. Williams, A. Miller, Transporters responsible for the uptake and partitioning of nitrogenous solutes. *Annu. Rev. Plant Physiol. Plant Mol. Biol.* **52**, 659–688 (2001).
51. D. Wipf *et al.*, Conservation of amino acid transporters in fungi, plants and animals. *Trends Biochem. Sci.* **27**, 139–147 (2002).
52. L. K. Kang, T. A. Rynearson, Identification and expression analyses of the nitrate transporter gene (NRT2) family among Skeletonema species (Bacillariophyceae). *J. Phycol.* **55**, 1115–1125 (2019).
53. B. Guo *et al.*, Characterization of the nitrate transporter gene family and functional identification of HvNRT2.1 in barley (*Hordeum vulgare* L.). *PLoS One* **15**, e0232056 (2020).
54. C. Luschnig, R. A. Gaxiola, P. Grisafi, G. R. Fink, EIR1, a root-specific protein involved in auxin transport, is required for gravitropism in *Arabidopsis thaliana*. *Genes Dev.* **12**, 2175–2187 (1998).
55. J. Friml *et al.*, AtPIN4 mediates sink-driven auxin gradients and root patterning in Arabidopsis. *Cell* **108**, 661–673 (2002).
56. J. Friml *et al.*, Efflux-dependent auxin gradients establish the apical-basal axis of Arabidopsis. *Nature* **426**, 147–153 (2003).
57. G. Brunoud *et al.*, A novel sensor to map auxin response and distribution at high spatio-temporal resolution. *Nature* **482**, 103–106 (2012).
58. A. Colón-Carmona, R. You, T. Haimovitch-Gal, P. Doerner, Technical advance: spatio-temporal analysis of mitotic activity with a labile cyclin-GUS fusion protein. *Plant J.* **20**, 503–508 (1999).
59. I. Blilou *et al.*, The PIN auxin efflux facilitator network controls growth and patterning in Arabidopsis roots. *Nature* **433**, 39–44 (2005).